19th Australasian Fluid Mechanics Conference
Melbourne, Australia
8-11 December 2014

The Effect of Length to Height Ratio on the Wake Structure and Surface Pressure of a High-Speed Train

J.R. Bell[1], D. Burton[1], M. C. Thompson[1], A. Herbst[2] and J. Sheridan[1]

[1] Department of Mechanical & Aerospace Engineering, Monash University, Australia.
[2] Centre of Competence for Aero- and Thermodynamics, Bombardier Transportation, Sweden.

Abstract

An experimental investigation into the effect of reduced length to height ratio - a limitation both experimentally and numerically - has on the wake and tail surface pressure of a high-speed train has been undertaken to better understand the induced flow. Presented are boundary layer measurements at the tail, velocity mapping of the time averaged wake, and the surface pressure distribution at the train tail for 4 physical train lengths and 3 artificial train lengths utilising boundary layer augmentation.

Introduction

High-speed trains (HSTs) have a number of aerodynamic characteristics that are important to their operation: drag, head pressure pulse, crosswind stability and slipstream. The length to height ratio (L/H) of a typical high-speed train is 25-50. This is difficult to model experimentally, due to test section size limitations in wind tunnels as well as numerically, as large domains are computationally demanding. The work presented is an investigation into the sensitivity of the time-averaged near-wake topology of a HST has to the L/H. This work is part of a larger investigation into the sensitivity of slipstream and transient near wake features of a HST to L/H.

The induced flow known as 'slipstream' caused by a HST's motion through air can be hazardous to commuters at platforms, track-side workers and infrastructure. As such a HST's slipstream performance is regulated in Europe. Full-scale experiments have shown the highest slipstream velocities occur in the near wake of a HST[1]. The presence of twin counter-rotating longitudinal vortices in the near wake of a HST has been previously associated with the largest slipstream velocities by the authors [2].

An experimental investigation by the authors [3] in a moving model provided inconclusive evidence of sensitivity of longitudinal slipstream profiles to two different lengths investigated (L/H=12 and 16). Muld et al. [4] numerically investigated the effect L/H has on the flow structure and surface pressure distribution over the tail with a Delayed Detached Eddy Simulation (DDES) and the use of Proper Orthogonal Decomposition (POD) of an ICE2 HST at a Reynolds number of 50,000. They observed that for the 3 lengths investigated (L/H= 12.5, 18.75, 25) that the first five individual POD modes and the reconstructed flow field based on these modes was insensitive to L/H. However, the dominant frequencies of these primary modes were found to be sensitive to L/H. Surface pressure distribution over the tail was also relatively insensitive, with similarity of the key features; however, it was observed that higher surface pressure occurred on the roof of the tail for the larger L/H, while the lower L/H exhibited higher pressure on the tail close to the tip.

The sensitivity of the wake structure, and thus the slipstream of a HST to L/H has been acknowledged in the literature and partially investigated, yet has not been explicitly explained and thus confidence in slipstream predictions using reduced L/H can be improved. The work presented aims to add to this understanding, as it investigates the relationship between time-averaged flow structure and tail surface pressure distribution to L/H, including boundary layer measurements at the tail to quantify the influence that L/H has upstream of the tail. This is undertaken with a model with 4 physical lengths and 3 artificial train lengths utilising boundary layer augmentation.

Methodology

A 1/10th scale model of an ICE3 - a high-speed train in operation throughout Germany - was used in the experiment. The model measured 5×0.3×0.4m (L×W×H), with a cross-sectional area of 0.115m^2. Roof boundary layer experiments were performed in the Monash University large (1.4MW) open-jet wind tunnel, with working section (12×2×4m: L×W×H), resulting in a blockage ratio of 2%. Flow mapping of the wake and surface pressure measurements were performed in the Monash Universitiy (450kW) closed-jet wind tunnel, (14×2×2m: L×W×H),resulting in a blockage ratio of 7%. The Reynolds number based on width was 7.2×10^5 for both experiments, with both test sections fitted with a splitter plane to reduce the effect of the wind tunnel ground boundary layer (see Figure 1). Comparison of time-averaged flow mapping in the *YZ* plane at *X*=1H for the standard scenario of L/H=14 in both wind tunnels, indicated differences in the experimental set-up had negligible effects on these particular results.

The model had 4 sets of bogies with no inter-carriage gaps, and was mounted above a 1/10th scale single-track ballast and rail (STBR) ground configuration. The STBR leading edge had a front angle of 37^o equivalent to the side angle, and was swept 180^o. Separate tests with a cobra probe as below found no separation occurred over the leading edge of the STBR.

The length of the ICE3 model was altered to achieve L/H ratios of 6,9,11,14, with larger L/H simulated by augmenting the boundary layer development over the surface of the train in three ways: a 0.035H (14mm) high fence, and 0.125H and 0.25H (50, 100m) high spire trips, placed around the circumference of the model. These trips were placed at location A in Figure 1, 2.5H from the train's nose. The width-to-height ratio of the spires was 0.3 with no gap between tips.

The boundary layer on the roof at the rear of the train at *x*=-2.5H (dotted line in Figure 1) was measured for each scenario with a 4-hole dynamic pressure probe (cobra type). This measurement position was sufficient distance from the tail so that no tail effects - acceleration over the roof - were visible. Sample times were 15 seconds and taken at a sampling frequency of $1000Hz$. All velocity measurements were normalized by an upstream reference pitot-static tube corrected to the models location with a dynamic pressure factor. The boundary layer, displacement and momentum thickness for all scenarios were calculated with Equations 1, 2 and 3 respectively.

$$\delta = z \quad when \quad U(z) = 0.99U_\infty, \tag{1}$$

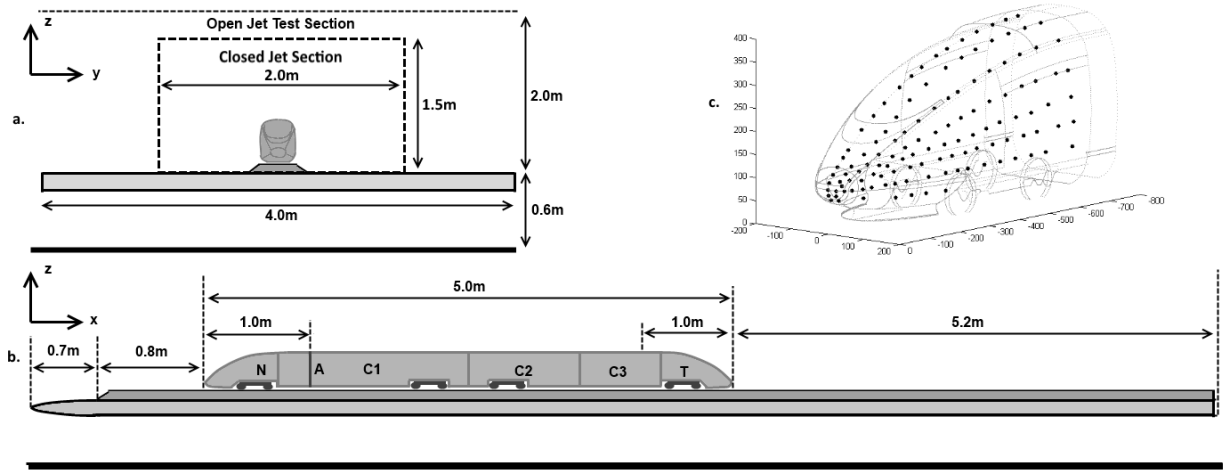

Figure 1: Experimental Setup. a) Front view, with reduced test section of closed jet section indicated by dotted square. b) Side view, showing train removable sections, tripping location(A) and roof boundary layer measurement position (dashed line). c) 122 Tap locations on right hand side of tail surface.

$$\delta^*(x) = \int_0^\infty \left(1 - \frac{U}{U_\infty}\right) dy, \tag{2}$$

$$\theta(x) = \int_0^\infty \frac{U}{U_\infty}\left(1 - \frac{U}{U_\infty}\right) dy. \tag{3}$$

Flow mapping in the near wake in the *YZ* (spanwise) plane at *X*=1H (one train height downstream of the tail) using cobra probes obtained the time averaged wake for each case. The *u* component (velocity in the streamwise direction) was converted to the 'induced' component (that which a stationary observer would experience) through Equation 4. The freestream velocity u_∞ was determined by an upstream reference pitot-static tube as described above. Vorticity, Γ_2 and Γ_1 are used as vortex identifiers [5] in the near wake and were determined for each scenario tested from the three components of velocity calculated from the cobra probe.

$$\mathrm{u}_{induced} = 1 - \frac{u}{u_\infty}. \tag{4}$$

Surface pressure over one half of the model's tail was measured using 122 pressure taps (see Figure 1c). Data was measured at all points simultaneously at a sampling rate of 2000Hz. The length of the tubing from the probes to the transducers was 1.5m enabling an acceptable frequency response below 300Hz with corrections for phase and amplitude distortion. Results are presented as the coefficient of pressure (Equation 5), for the standard case (L/H=14) and the percentage change in pressure from the standard case for all others (Equation 6).

$$\mathrm{C}_P = (P_i - P_{static,ref})/(P_{total,ref} - P_{static,ref}), \tag{5}$$

$$\Delta C_P\% = 100 * (C_{P,Scenario,Tap} - C_{P,LH14,Tap})/C_{P,LH14,Tap}. \tag{6}$$

Results

Boundary Layer

The boundary layer profiles for each scenario are presented in Figure 2. There is smooth progression of the boundary layer profiles for the four different lengths. A large increase in boundary layer profile occurs for the 14mm trip, with the following two spires showing a similar size difference to the profile for each increase in height. The boundary layer thickness, momentum thickness and displacement thickness for all cases are presented in Table 1; this provides a level of quantification to the differences between scenarios tested.

These results show a large variation in the boundary layer thickness at the tail existed for the different scenarios, thus provides a good basis in which to assess the effect of the boundary layer has on the near wake flow structure.

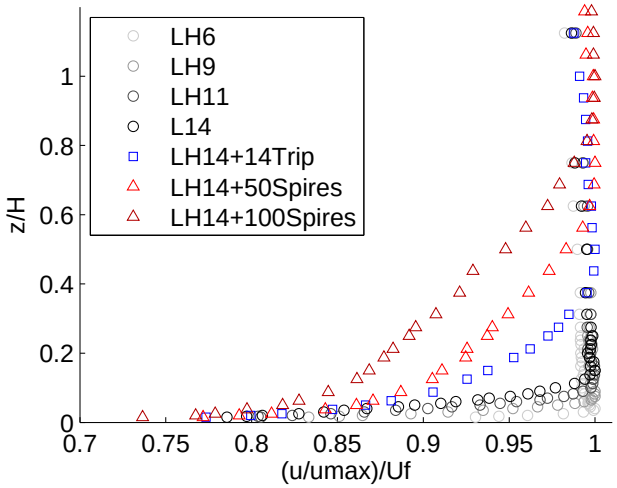

Figure 2: Boundary layer velocity profiles @X=-2.5H.

	δ/H	δ^*/H	Θ/H
L/H:6	0.0280	0.0014	0.0013
L/H:9	0.0550	0.0051	0.0045
L/H:11	0.0850	0.0082	0.0071
L/H:14	0.1200	0.0110	0.0095
L/H:14+14T	0.3200	0.0220	0.0200
L/H:14+50S	0.5400	0.0360	0.0320
L/H:14+100s	0.7800	0.0630	0.0550

Table 1: Boundary layer thickness, displacement thickness and momentum thickness on the roof @X=-2.5H.

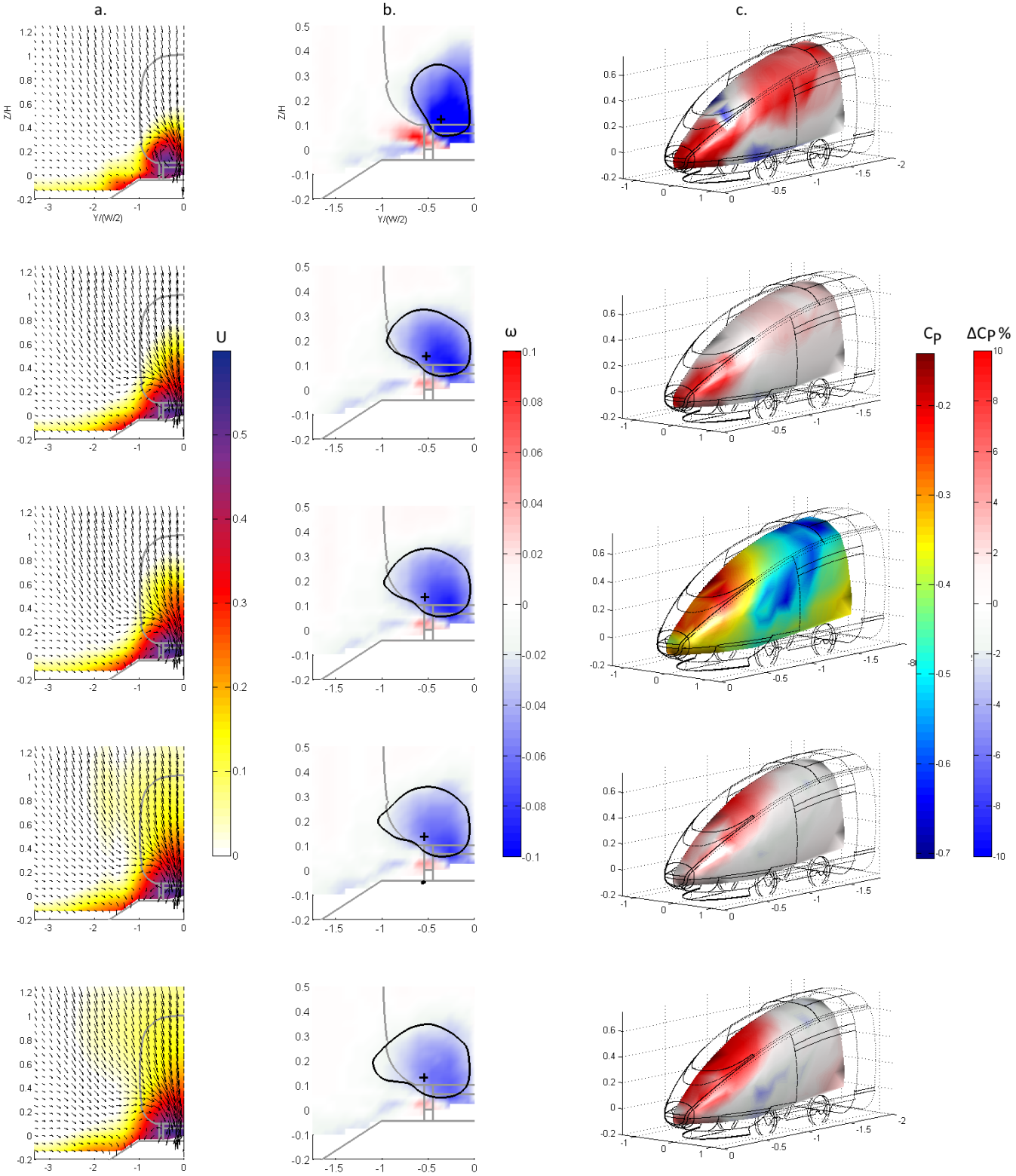

Figure 3: Top to bottom: L/H:6,11,14, 14+0.125H (50mm) Trip,14+ 0.25H (100mm) Trip. YZ slices @X=1H. a)Contour of induced u velocity with v,w vectors. b) Vorticity contours overlaid with contour line of Γ_2=2/pi, Γ_1 max indicated by +. c) C_P distribution (middle figure), all others ΔC_P%

Time Averaged Wake

The results from the flow mapping performed with the 4-hole dynamic pressure (Cobra) probes are presented in Figure 3a and b. The induced velocity field in the *YZ* plane at *X*=1H is seen in Figure 3a, where *u* is displayed as filled coloured contours and v,w are overlaid as vectors. The presence of the key feature of the near wake, the longitudinal vortex (one of a symmetrical pair) is consistent in both magnitude of *u* and location of the vortex visible in the vectors for all scenarios.

However, there are two main points of difference that indicate the L/H does have some effect on the near-wake topology. For the L/H=6 scenario, the vortex core has higher *u* magnitudes, and from the vectors is visibly closer to the centreline. Further, both the 0.125H and 0.25H spire scenarios show a development region over the roof with a larger induced *u* component. This region of induced flow of *u*=0.1 does not reach down to the sides of the train, where below *Z*=0.4H the contours remain constant for all scenarios excluding L/H=6. This has important implications for slipstream results, as a stationary observer or infrastructure only experiences the flow beyond the passage of the vehicle and generally between *Z*=-0.2 to 0.5H.

The vorticity, $\Gamma_2 = 2/\pi$ contour lines and maximum of Γ_1 in Figure 3b, are used to identify the longitudinal vortex[5] and the effect of L/H on this structure. Similarly to the velocity results, the L/H=6 case has a smaller vortex, closer to the centreline with the most concentrated vorticity. The effect of increasing L/H beyond L/H=6 is not large, however there is a trend for the region determined by $\Gamma_2 = 2/\pi$ to increase in size slightly, and peak away from the centreline, together with a decrease in the concentration of vorticity. The location of the maximum Γ_1 is consistent for all cases excluding L/H=6.

These results compare well in principle to those of Muld et al[4], as the key features of the wake topology are consistent regardless of L/H. However, the trend for the vortex to increase in size with less concentrated vorticity indicates that there may be more significant differences in the topology further downstream from the tail. Previous work by the authors have found the near wake maximum in the slipstream velocity is associated to the vortex moving outwards beyond the vehicles width to where slipstream would affect a person; the position of the peak is dependant on the height being measured, but occurs in the range of *X*=3H to 10H.

Surface Pressure Distribution

The pressure distribution over the tail of the model is shown in Figure 3c, with the middle plot being the pressure distribution, while above and below represent the difference in pressure from that case. Considering the middle plot showing the pressure distribution over the tail, a band of low pressure can be observed over the roof and around the sides. This is likely due to the accelerated flow over this area as the air curves around the tail into the wake. The other main feature is the region of higher pressure on the tail, an explanation for this is the strong downwash that occurs in this area, which is evident from Figure 3a. In this high pressure region, a distinction is visible either side of the wiper region, where the lines indicate where the wiper housing feature steps up off the surface. This explains the higher pressure at the front and the reduced pressure downstream of this geometry. The lower pressure around the tip of the tail likely indicates where the flow separates.

No effect of the L/H on surface pressure was visible through direct comparison of surface pressure distributions, thus the difference is plotted, with maximum of $\pm 10\%$. Thus, the magnitudes of the differences due to L/H are not large, however some trends are visible. For the smaller L/H, a larger pressure at the tip of the tail is seen; for L/H=6 specifically the difference over the roof and influence of the wiper blade are distinct. An explanation for this is that the boundary layer is smaller over the surface, the influence of wiper would be larger, and the flow is more likely to stay attached to the tail tip, thus resulting in higher pressure. For the larger L/H, where only the two spire cases are shown of the augmented scenarios, the high pressure region visible in the standard L/H=14 figure increases with increasing L/H. These two trends of increasing pressure at the tail tip for shorter L/H, and increasing pressure over the roof for longer L/H, are similar to the results of Muld et al even given the significant difference in Reynolds number (Re: 50,000 numerically to 700,000 presented here).

Conclusions

This work is a first step towards understanding the effect a reduced L/H model will potentially have on the slipstream of a high-speed train. The time-averaged near-wake topology and surface pressure are useful in identifying the cause of any differences in slipstream predictions, which are the longitudinal profiles of induced velocity as a stationary observer would experience. Time-averaged flow mapping further downstream in the wake would be beneficial to see if the minor trends visible with increasing L/H are amplified, or if the effects are limited to the near wake.

These results are a subset of a larger experimental program which includes analysis of the transient wake as well as direct comparison of longitudinal slipstream profiles. These results together will provide an answer sd to whether L/H has an effect on slipstream and if it does, to provide some insight into the feasibility of boundary layer augmentation as a a means of artificially increasing the effective L/H of the model in order to predict the slipstream of full length operational trains more accurately.

Acknowledgements

The Faculty of Engineering, Monash University is acknowledged for the Engineering Research Living Allowance stipend scholarship for J.R. Bell.

References

[1] Baker, C., Quinn, A., Sima, M., Hoefener, L. and Licciardello, R. Full scale measurement and analysis of train slipstreams and wakes: Part 1 ensemble averages. Proc. Institute of Mechanical Engineers Part F: Journal of Rail and Rapid Transport, **228(5)**, 2014, 451-467.

[2] Bell, J.R., Burton, D.,Thompson, M., Herbst, A. and Sheridan, J. Wind tunnel analysis of the slipstream of high-speed trains. Proceedings of International Workshop on Railway Aerodynamics, Birmingham, UK, 2013.

[3] Bell, J.R. and Herbst, A. Moving model analysis of the slipstream of high-speed trains. Proceedings of International Workshop on Railway Aerodynamics, Birmingham, UK, 2013.

[4] T. Muld, G. Efraimsson, and D.S. Hennigson. Wake characteristics of high-speed trains with different lengths. Journal of Rail and Rapid Transit, **228(4)**, 2014, 333–342.

[5] L. Graftieaux, L., Michard, M. and Grosjean, N. Combining PIV, POD and vortex identification algorithms for the study of unsteady turbulent swirling flows. Journal of Measurement Science and Technology, **12**, 2001, 1422–1429